Electronic supporting information

Porosity-driven Large Amplitude Dynamics for Nitroaromatics Sensing with Fluorescent Films of Alternated D-π-A Moleculess

Jean-Pierre Malval*[1], Marion Cranney[1], Sylvain Achelle *[2], Huriye Akdas-Kiliç [2], Jean-Luc Fillaut [2], Nolwenn Cabon[2], Françoise Robin-le Guen [2], Olivier Soppera1, Yann Molard[2].

[1] Institut de Science des Matériaux de Mulhouse CNRS-UMR 7361, Université de Haute Alsace, 15 rue Jean Starcky, 68057, Mulhouse, France.
[2] Université de Rennes, Institut des Sciences Chimiques de Rennes CNRS UMR 6226, F-35000 Rennes.

Correspondence to:
J.-P. Malval (e-mail : jean-pierre.malval@uha.fr) and
S. Achelle (e-mail : sylvain.achelle@univ-rennes1.fr)

CONTENTS

1. Figures and Tables.

	media	λ_{abs} (ε_{abs}) / nm (10^3 M^{-1} cm^{-1})	λ_{fluo} / nm	Φ_{fluo}	τ_{fluo} / ns	k_r ^{c} / 10^9 s^{-1}	k_{nr} ^{c} / 10^9 s^{-1}
MON	TOL	430 (47.6)	478	0.85	2.16	0.39	0.07
	Film [a]	439	532	0.18	0.89 [b]	0.20	0.92
MOL	TOL	428 (49.6)	476	0.81	2.15	0.37	0.09
	Film [a]	436	514	0.22	1.05 [b]	0.21	0.74

[a] The film thickness of **MON** and **MOL** is 40 ± 5Å. [b] Averaged fluorescence lifetime from a 3 exponentials fitting time decay. [c] $k_r = \Phi_f / \tau_f$ and $k_r = (1- \Phi_f) / \tau_f$

Table S1. Photophysical data of compounds in toluene and spin-cast films.

		λ_{abs} / nm	λ_{fluo} / nm	Φ_{fluo}	τ_{fluo} / ns	k_r / 10^9 s^{-1}	k_{nr} / 10^9 s^{-1}
MON	TOL	430	478	0.85	2.16	0.39	0.07
	THF	428	553	0.84	2.21	0.38	0.07
	DCM	432	555	0.92	2.90	0.32	0.03
	ACN	423	595	0.75	1.93	0.39	0.13
MOL	TOL	428	476	0.81	2.15	0.37	0.09
	THF	429	546	0.80	2.17	0.37	0.09
	DCM	434	550	0.88	2.67	0.33	0.04
	ACN	428	594	0.61	2.05	0.30	0.19

[a] $k_r = \Phi_f / \tau_f$ and $k_{nr} = (1-\Phi_f) / \tau_f$

Table S2. Photophysical data of compounds in various solvents.

	E_{ox}^{1} / V *vs.* SCE	E_{ox}^{2} / V *vs.* SCE
MON	0.83	1.04
MOL	0.88	1.09

Table S3. Redox potentials of chromophores in acetonitrile + $TPAPF_6$ (0.1 M) on platinum electrode at 100 mV s^{-1}.

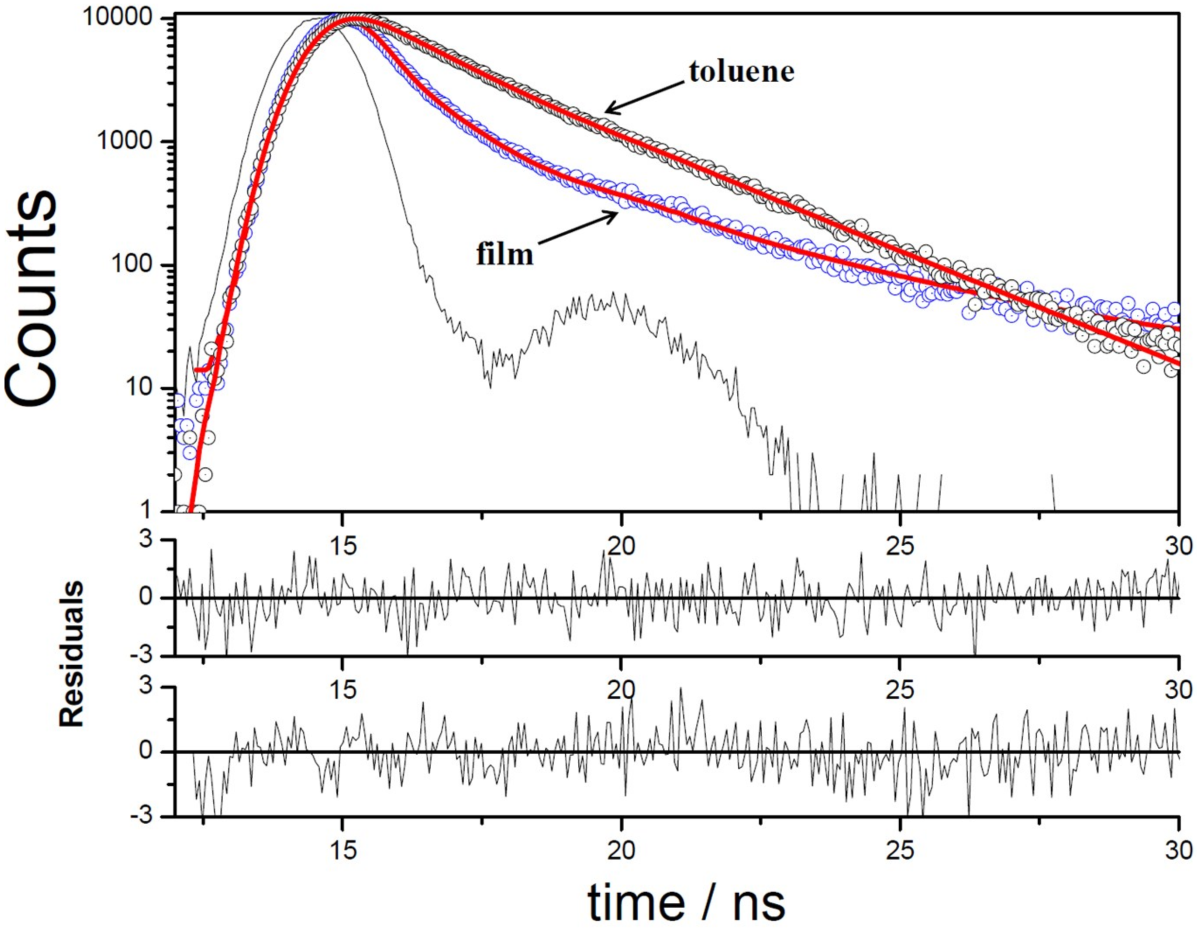

Figure S1. Fluorescence decays of **MON** in toluene and in spin-cast film. The fluorescence emission was collected at the maximum emission wavelengths. The residual graphs are displayed at the bottom and correspond to a monoexponential and three-exponential fits for **MON** in toluene and spin-cast film respectively.

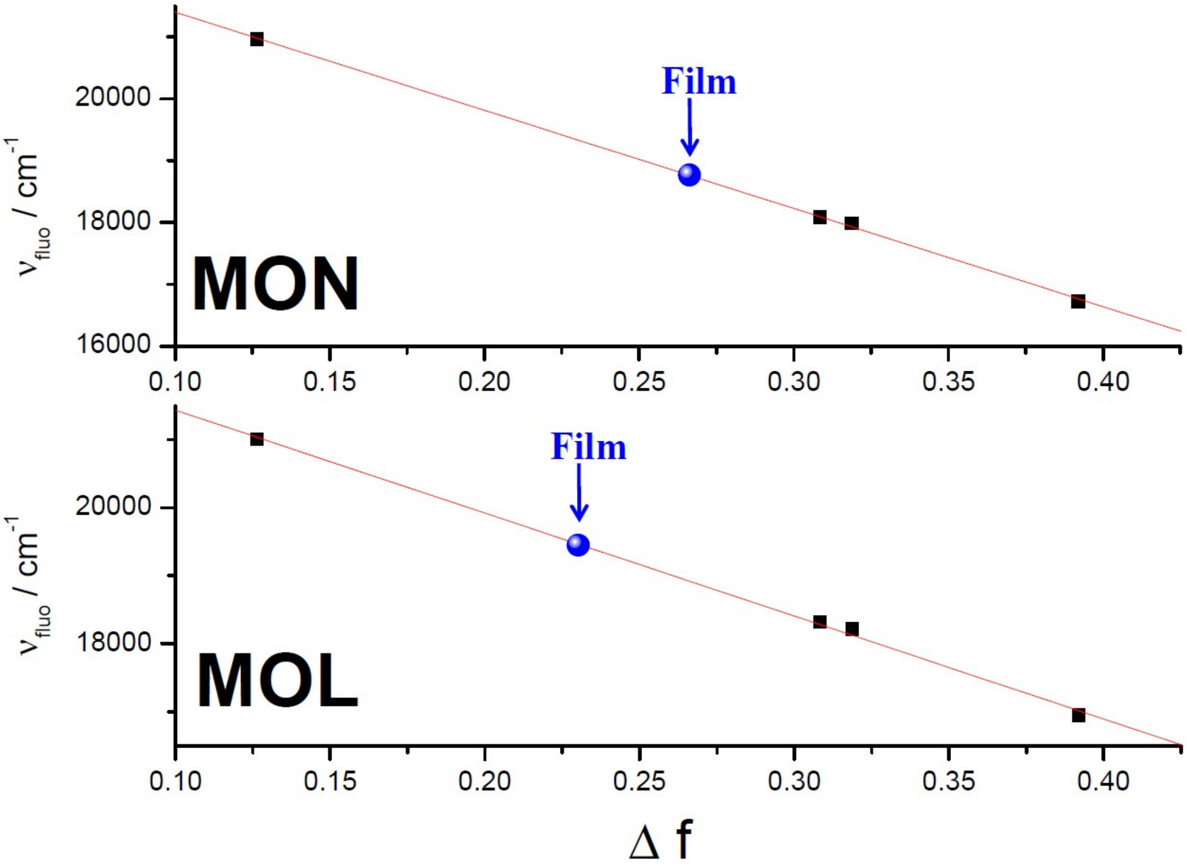

Figure S2. Solvatochromic plots of the fluorescence maximum wavenumbers (ν_f^{MAX}) of chromophores as function of the Lippert-Mataga solvent polarity function, f(ε,n). Note that the ν_f^{MAX} of each chromophore in spin-cast film has been positioned on the solvatochromic plots to estimate the corresponding Δf.

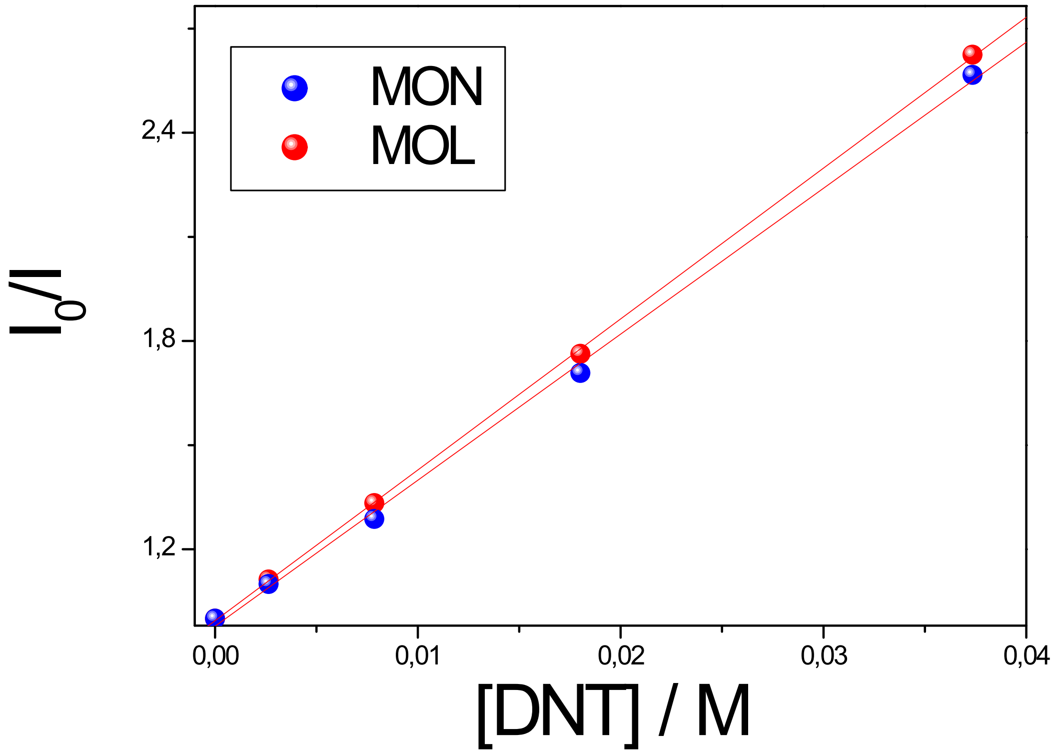

Figure S3. Stern-Volmer plots of the fluorescence quenching of chromophores by DNT in acetonitrile.

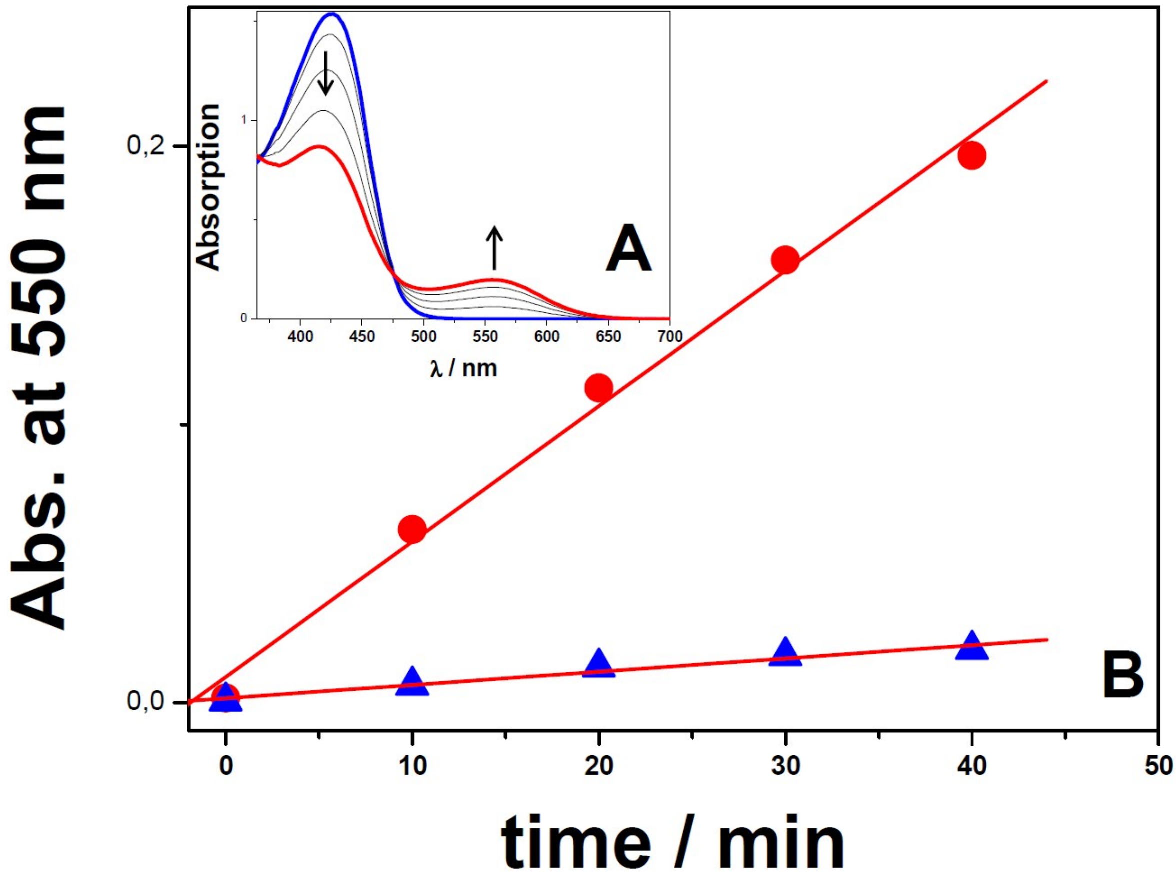

Figure S4. **A.** Evolution of the absorption spectrum of **MOL** (3×10^{-5} M) in N_2-saturated ACN mixed with a large excess of DNT (3×10^{-3} M) during photolysis at λ_{irr} : 436 nm. **B.** Comparison of the time-dependent absorbance changes at 550 nm during the irradiation of ACN solutions containing **MOL**: without DNT (triangles) and with DNT (circles).

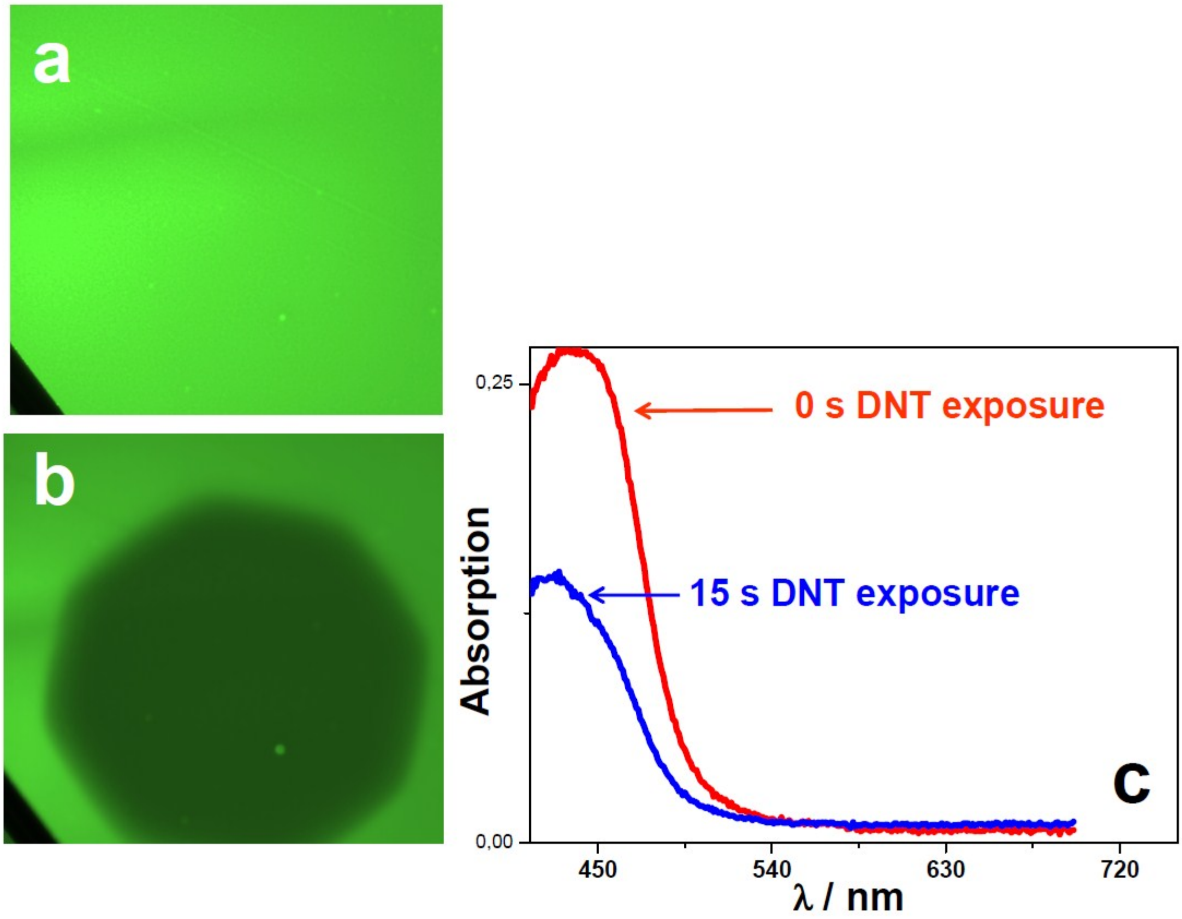

Figure S5. Epifluorescence images of spin cast film of **MOL** : **(a)** after 5 min excitation at 365 nm under N_2 stream **(b)** after 15 s excitation at 365 nm under DNT vapors exposure. Note that the octagonal dark area in image b denotes the excitation zone. **(c)** Absorption spectrum of **MOL** thin-film before and after exposure to DNT vapors.

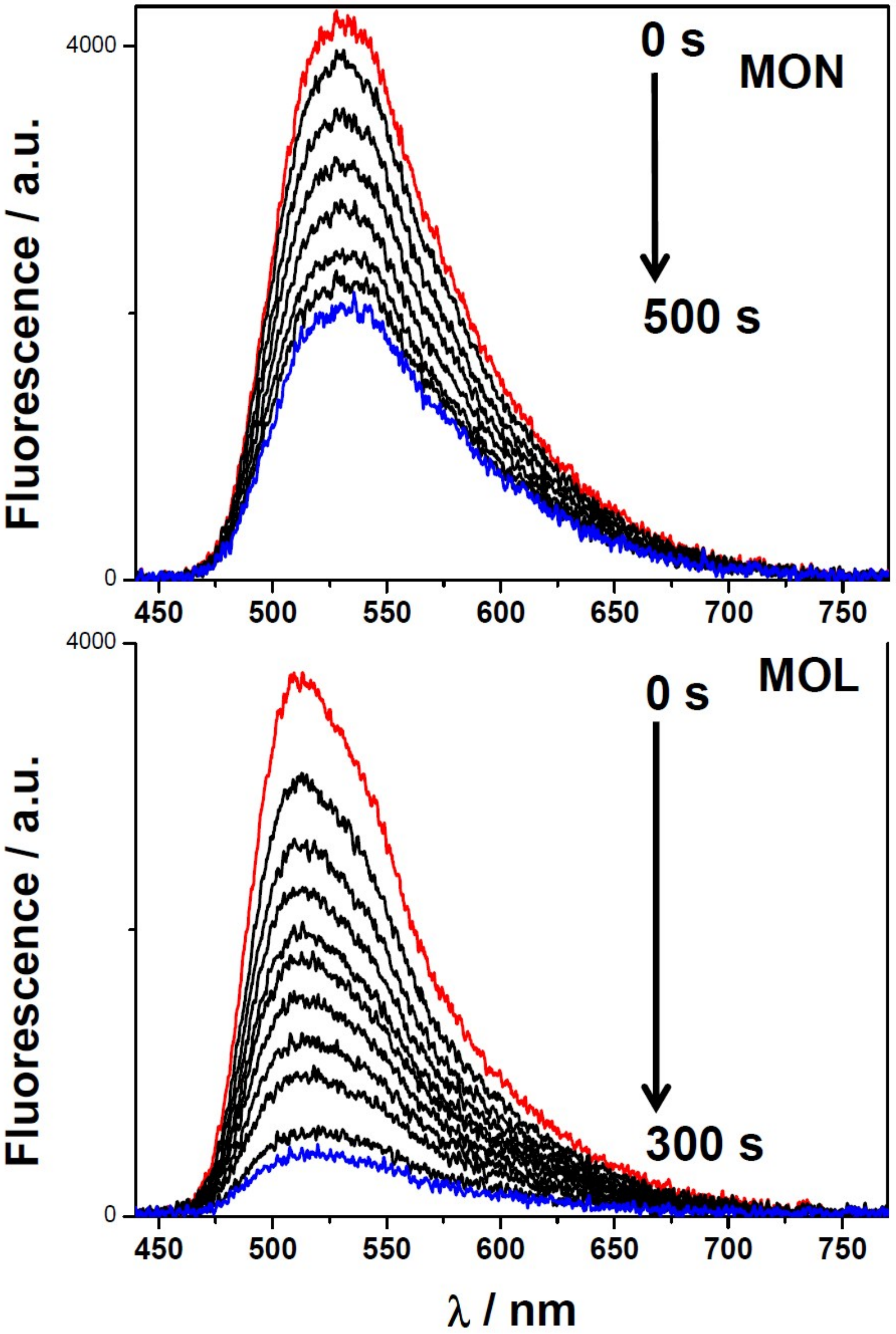

Figure S6. Time-dependent fluorescence spectra of spin-cast films of chromophores exposed to DNT vapors.

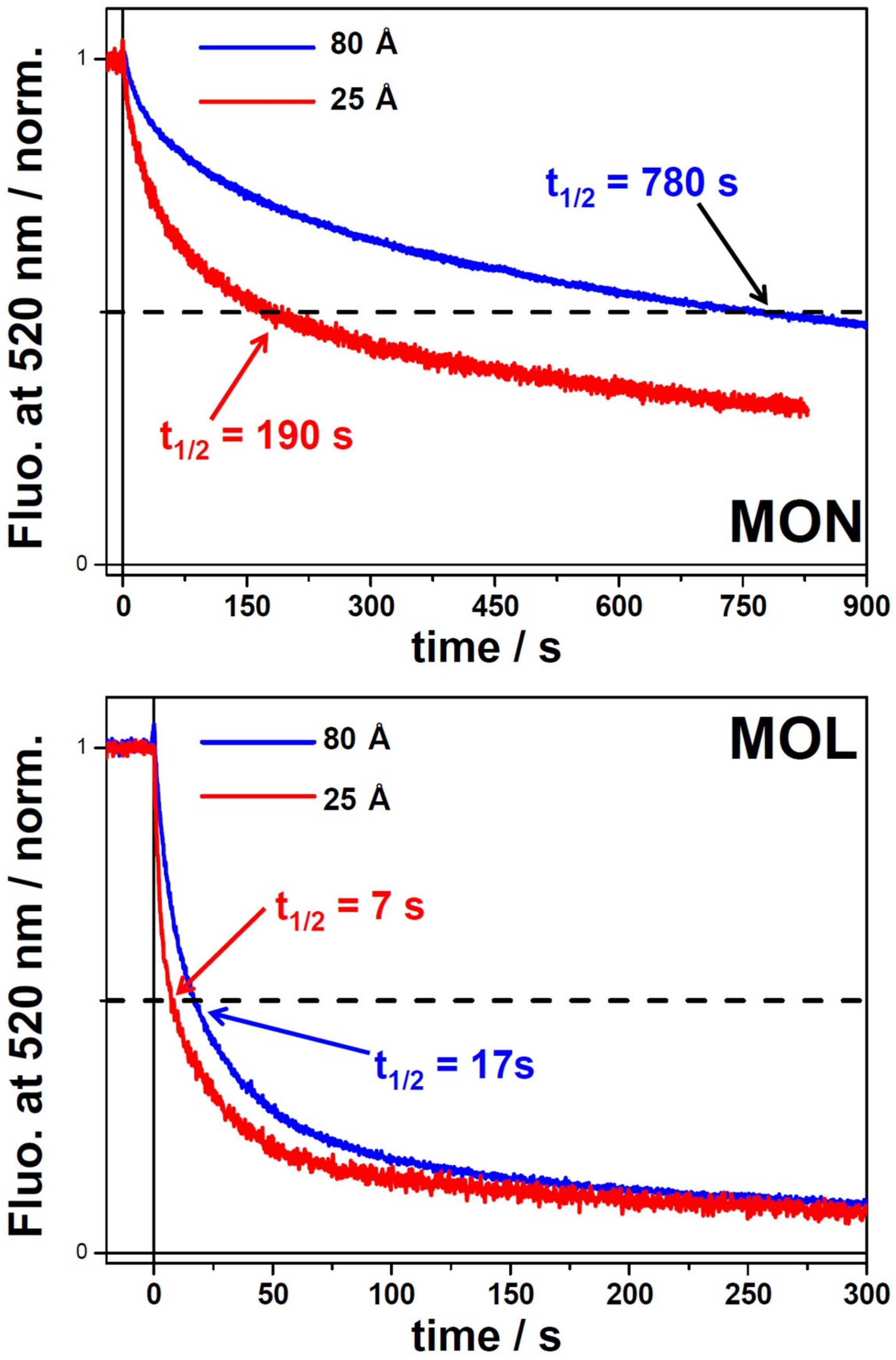

Figure S7. Time-dependent fluorescence intensity changes of chromophores in 25-Å and 80-Å films upon exposure to DNT vapors.

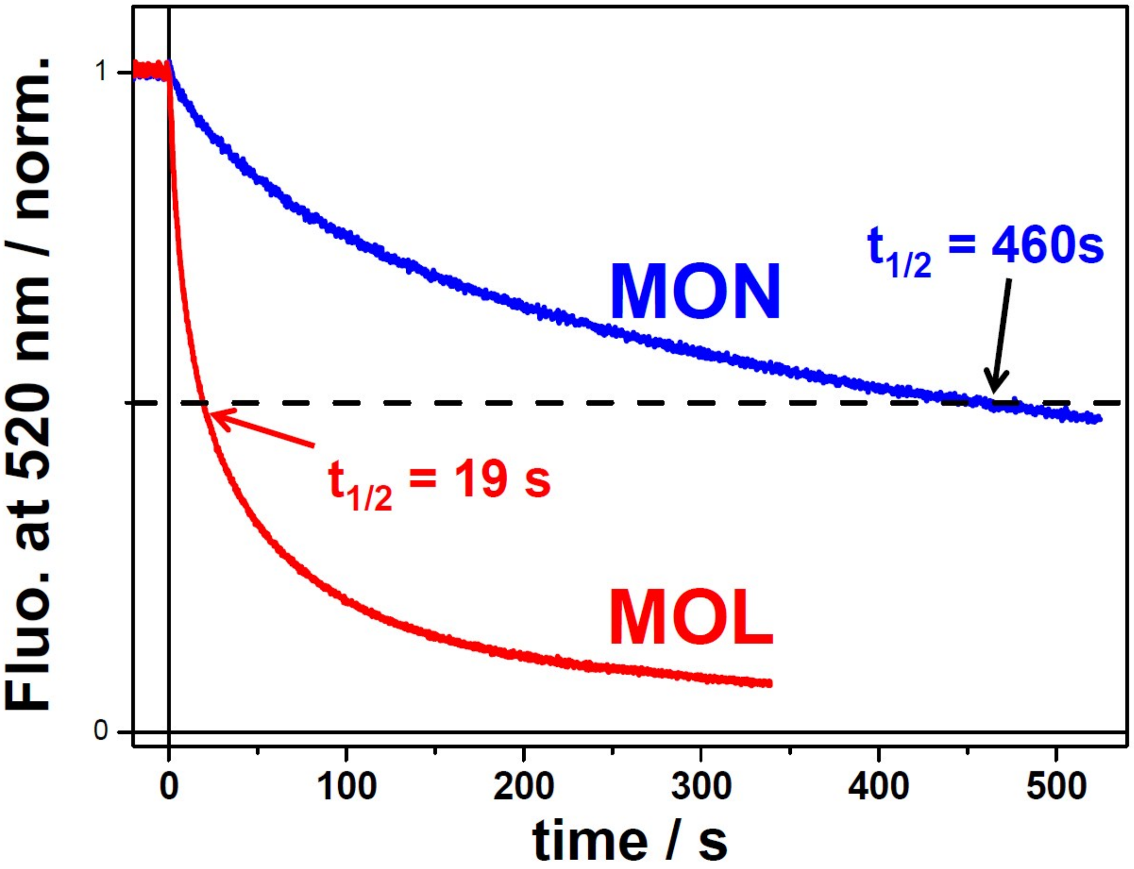

Figure S8. Fluorescence quenching kinetics of **MON** and **MOL** films exposed to a 300 mL min^{-1} N_2 flow with 2,6-DNT at a vapor pressure of ~ 200 ppb. Half-time for fluorescence quenching is also indicated for each film. Both films have a similar thicknesses of about 45 ± 5 Å.

2. Materials and General Characterization Methods.

Materials and general methods.

Materials. All the solvents employed were Aldrich spectroscopic grade. The absorption and fluorescence of all solvents were checked for impurities and have been subtracted from the sample spectra. Reagents for synthesis were purchased from commercial suppliers and used without further purification. 2,4-dinitrotoluene (DNT), 2,6-dinitrotoluene (2,6-DNT), 1-Phenyloctane (98% purity) were purchased from Aldrich.

NMR spectra were acquired at RT with a Bruker Advance 300 spectrometer. Chemical shifts are given in parts per million relative to TMS (1 H, δ=0.0 ppm) and $CDCl_3$ (13 C, δ=77.0 ppm). Acidic impurities in $CDCl_3$ were removed by treatment with anhydrous K_2CO_3. High resolution mass analyses were performed by using a Bruker MicroTOF-Q II apparatus.

Steady-state absorption and luminescence spectra. The absorption measurements were carried out with a Perkin Elmer Lambda 2 spectrometer. Steady-state fluorescence spectra in solution were collected from a FluoroMax-4 spectrofluorometer. Emission spectra are spectrally corrected, and fluorescence quantum yields include the correction due to solvent refractive index and were determined relative to quinine bisulfate in 0.05 molar sulfuric acid (Φ = 0.52)[1]. The absolute fluorescence quantum yields of thin-films were measured using an integrating sphere (C9920-02 from Hamamatsu) equipped with a 150 W Xenon light source, an excitation monochromator and a CCD spectrometer (PMA-12) for the simultaneous luminescence collection in the 350-1100 nm range.

Photolysis reactions. The photolysis of the chromophores in ACN in presence of DNT was carried out under continuous irradiation at 436 nm using an Hg-Xe lamp (LC 9588/01A from Hamamatsu) equipped with a band pass filter centred at 440 nm (FB440-10 from Thorlabs). The progress of the reaction was monitored via the absorbance change using a Perkin Elmer Lambda 2 spectrometer. Experiments were performed at 25°C in N_2-degassed solutions which were continuously stirred.

Time-correlated single-photon counting. The fluorescence lifetimes were measured using a Nano LED emitting at 372 nm as an excitation source with a nano led controller module, Fluorohub from IBH, operating at 1MHz. The detection was based on an R928P type photomultiplier from Hamamatsu with high sensitivity photon-counting mode. The decays were fitted with the iterative reconvolution method on the basis of the Marquardt/Levenberg algorithm[2]. Such a reconvolution technique allows an overall-time resolution down to 0.2 ns. The quality of the exponential fits was checked using the reduced χ^2 (≤ 1.2).

Cyclic voltammetry. The cyclic voltammetry experiments[3] (using a computer-controlled Radiometer Voltalab 6 potentiostat with a three-electrode single compartment cell; the working electrode was a platinum disk; a saturated calomel electrode (SCE) used as a reference was placed in a separate compartment with a salt bridge containing the supporting electrolyte) were performed at 300 K, in N_2-saturated acetonitrile with a constant concentration (0.1 M) of n-Bu_4NPF_6 ($TBAPF_6$). Ferrocene (Fc) was used as an internal reference.

Spectroelectrochemistry. The spectroelectrochemical measurements were carried out method using a sealable PEEK-based microcell in 3-electrode configuration purchased from Rhd Instruments GmbH (Type: TSC Spectro). The working electrode consists in platinum gauze electrode inserted between two integrated quartz windows defining an optical length of 500 µm. A platinum disk (6 mm diameter) and a silver wire are used respectively as the counter electrode and the pseudo reference electrode. For potential calibration, ferrocene was used as internal standard. The spectroelectrochemical cell is optically connected using two optical fibers to a spectrometer (AvaSpec-ULS2048 from Avantes) and to a deuterium halogen compact light (AvaLight-DHc from Avantes). The same potentiostat used for cyclic voltammetry was used for spectroelectrochemistry. All the measurements were performed in N_2-saturated ACN in presence of 0.1 M of n-Bu_4NPF_6.

Scanning Tunneling Microscopy (STM). STM experiments at the solid-liquid interface were performed using a Nanoscope V Veeco working in ambient conditions with a Picoamp amplifier module and using a Pt-Ir tip immersed in the droplet. Images were acquired in constant current mode with the bias voltage applied to the sample. All STM images were processed with WSxM software by using plane levelling followed by background flattening with a correction of the drift using HOPG lattice[4]. The experiments were repeated several days using different tips to check for reproducibility, to avoid artefacts and to collect enough data in order to obtain pertinent and precise measurements. STM measurements were carried out at the solid-liquid interface on Highly Oriented Pyrolytic Graphite (HOPG). The 1-phenyloctane was used as non polar high boiling point solvent which does not compete with the adsorption process of the molecules on HOPG[5, 6]. The concentrations for **MOL** and **MON** in 1-phenyloctane were respectively of 7.6 mM and 2.1 mM. A droplet (500 µl) of each solution was deposited on a freshly cleaved surface of HOPG. We performed 29 (25) self-correlation measurements on STM images of self-assembled layers of **MOL** (**MON**) made when the drift of STM piezos was minimum.

Preparation of spin-cast films and thickness measurements. The thin films were prepared by spin coating method on glass coverslips (22 x 22 mm) using chloroform solutions of chromophores whose concentration was 8 mM for **MON** and 10 mM for **MOL**. The spin coating was performed at a spin rate of 3000 rpm using a Delta10TT photo resist spinner (Süss Microtec Lithography GmbH). Each sample was placed under vacuum overnight before use. The film thicknesses were measured by ellipsometry (UVISEL from Horiba Jobin Yvon) using spin-cast films prepared on silicon wafers with the same procedure used for thin films on glass substrates. For each compound, the thicknesses of five similar samples were measured leading to averaged values of ca. 42 ± 6 Å and 44 ± 5 Å for **MON** and **MOL** respectively.

Fluorescence Microscopy. The fluorescence signal of the excited spin-cast films was recorded using an Olympus IX73 inverted microscope equipped with a 75 W Xe lamp housing. The excitation of the films at 365 nm occurred through a 10X, 0.25-NA objective using a fluorescence mirror unit (U-FUN from Olympus) associating a band pass filter centered at 365 nm (BP360-370), dichroic mirror (DM410) and long pass filter (BA420IF). The epifluorescence signal from the spin-cast film is collected by the same objective, passes through the same fluorescence mirror unit and is either collected by a spectrometer (USB4000-UV-Vis Ocean Optics) or by a CMOS camera (ORCA-Flash4.0 from Hamamatsu). Neutral filters were placed on the excitation optical path of the microscope to attenuate the irradiation power which was adjusted to a value of 50 µW. Under this latter excitation condition, all the films placed under N_2 atmosphere remain photostable after more than 5 min continuous excitation.

Photoluminescence quenching upon exposure to DNT vapor. A home-built sample chamber was used to monitor the time-dependent fluorescence changes of the spin-cast films exposed to DNT vapors. A scheme of the chamber is displayed in **Figure S9A**. The spin-cast film is inserted at the bottom of the chamber which was placed onto the xyz platine of an inverted microscope which both allows the excitation of the film and its fluorescence signal collection as described in the previous paragraphs. The sample chamber which runs under a continuous 300 mL min^{-1} nitrogen flow was designed to have a reduced inner volume of about 1.2 mL in order to establish a quasi-instantaneous DNT vapor equilibrium upon introduction of a DNT pellet (diameter = 1 cm) clamped to the lid of the chamber. To guaranty a reliable reproducibility, each fluorescence quenching measurement upon DNT exposure was repeated three times with distinctive spin-cast films prepared in the same conditions. **Figures S9B-C** depict the corresponding kinetics for each chromophore. The resulting quenching half-times ($t_{1/2}$) were then averaged leading to $t_{1/2}$ values of 432 ± 21 s and 13 ± 2 s for **MON** and **MOL** respectively .

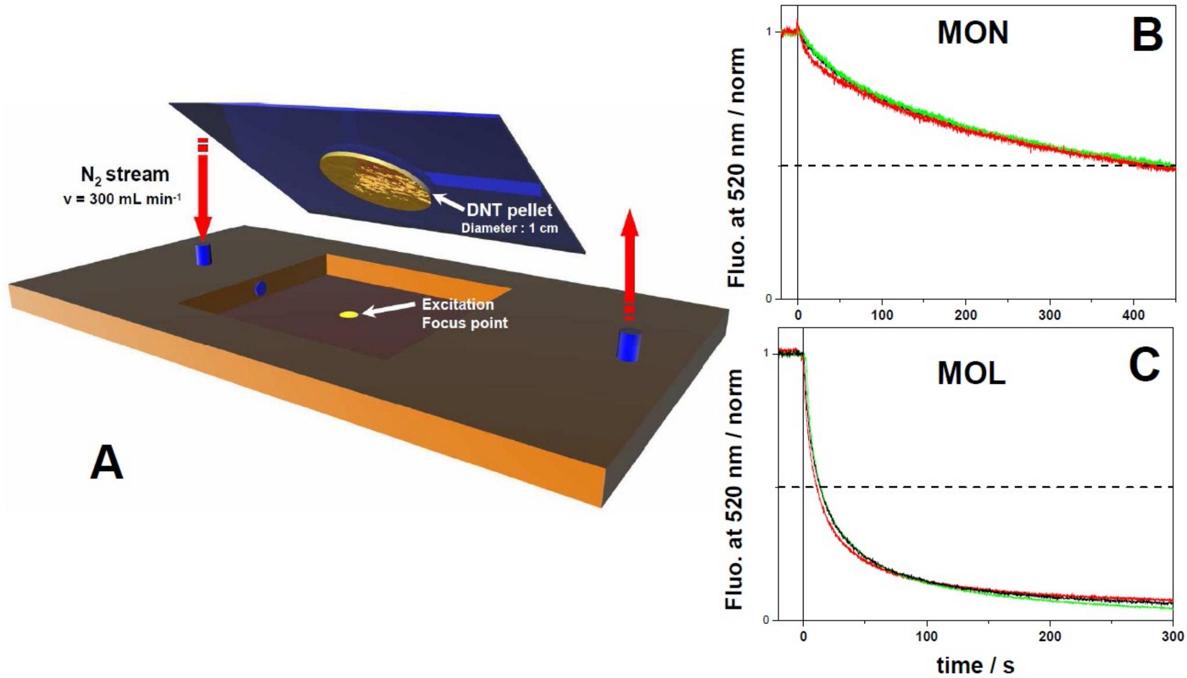

Figure S9. **A.** Scheme of the gas sample chamber. **B** and **C.** Time-dependent fluorescence intensity changes relative to three similar films for each compound exposed to DNT vapors.

The DNT and 2,6-DNT vapor pressures inside the chamber were determined by bubbling a known volume of analyte-infused N_2 through an acetonitrile solution whose absorption spectrum was recorded in UV-region using a long optical path cuve (l = 5 cm). With a fixed nitrogen flow rate of 300 mL min^{-1}, the nitroaromatics vapor pressures within the sample chamber have been estimated to values of ~ 60 ppb for DNT and ~ 200 ppb for 2,6-DNT at 25°C which are three times lower than their respective saturated vapors at the same temperature[7]. Finally, it should be emphasized that both compounds in film configuration are subject to photobleaching when irradiated under air atmosphere but remain perfectly photostable under nitrogen stream. As an example, **Figure S10** illustrates the fluorescence stability of a **MON** film excited more than five minutes at 365 nm under our microscope configuration.

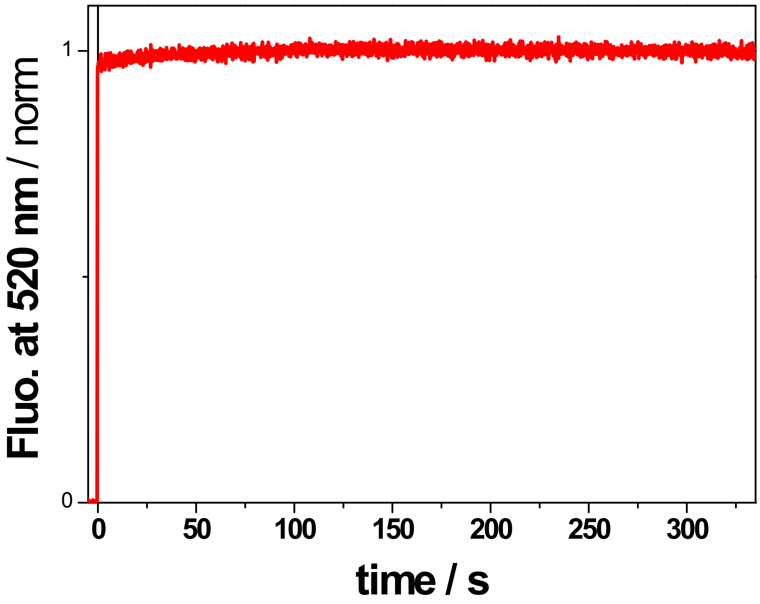

Figure S10. Photostability of the fluorescence of a **MOL** film under N_2 atmosphere and irradiated at 365 nm using a 10X, 0.25-NA objective (P = 50 μW)

3. Synthesis of chromophores.

4,6-distyrylpyrimidines **MOL** and MON have been obtained by Knoevenagel condensation of 4-diphenylminobenzaldehyde on the corresponding 4,6-dimethylpyrimidines according to reported procedure (**Scheme S11**).[8]

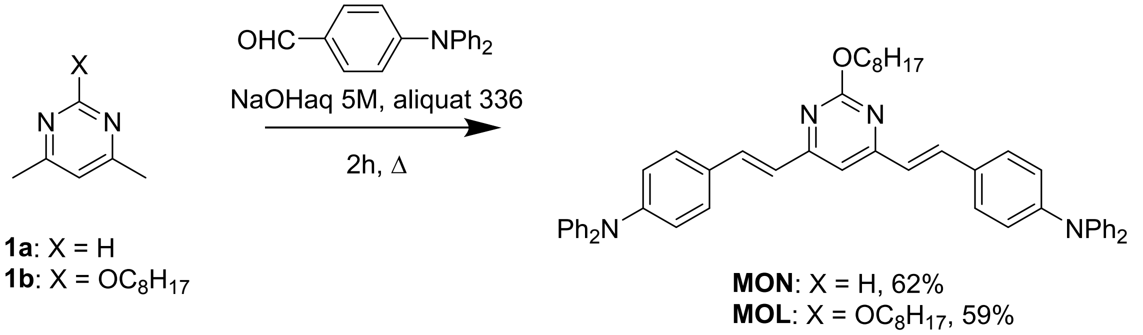

Scheme S1. Synthesis of **MOL** and **MON**.

4,6-bis((E)-4-(*N,N*-diphenylamino)styryl) pyrimidine (MON) has been obtained and characterized as described previously in reference [8].

4,6-bis((E)-4-(*N,N*-diphenylamino)styryl)-2-(octyloxy)pyrimidine (MOL): A stirred mixture of 4,6-dimethyl-2-(octyloxy)pyrimidine[9] (150 mg, 0.63 mmol) and 4-(*N,N*-diphenylamino)benzaldehyde (344 mg, 1.26 mmol) in aqueous sodium hydroxide (5M, 15 mL) containing Aliquat 336 (2 drops) was heated under reflux for 2h. The mixture was allowed to cool, and the filtrate was filtered off, washed with water and purified by column chromatography (SiO_2, petroleum Ether/EtOAc, 9:1). A yellow solid was obtained after trituration with Et_2O and pentane. Yield: 59% (276 mg). ^{1}H-NMR (300 MHz, $CDCl_3$): δ 0.84 (t, 3H, J = 7.2 Hz), 1.28-1.20 (m, 8H), 1.49-1.42 (m, 2H), 1.84-1.77 (m, 2H), 4.40 (t, 2H, J = 6.9 Hz), 6.80 (s, 1H), 6.83 (d, 2H, J = 15.3 Hz), 7.09–6.97 (m, 16H), 7.26–7.20 (m, 8H), 7.39 (d, 4H, J = 8.4 Hz), 7.79 (d, 2H, J = 16.2 Hz). ^{13}C-NMR (75 MHz, $CDCl_3$): δ 165.5 (C), 165.1 (C), 148.9 (C), 147.2 (C), 136.2 (CH), 129.4 (CH), 128.6 (CH), 125.1 (CH), 123.8 (CH), 123.6 (CH), 122.4 (CH), 110.5 (CH), 67.4 (CH_2), 31.9 (CH_2), 29.4 (CH_2) 29.3 (CH_2), 29.1 (CH_2), 26.1 (CH_2), 22.7 (CH_2), 14.1 (CH_3) HRMS (ESI/ASAP), *m*/*z* calculated for $C_{52}H_{51}N_4O$ $[M + H]^+$ 747.4057, found 747.4049.

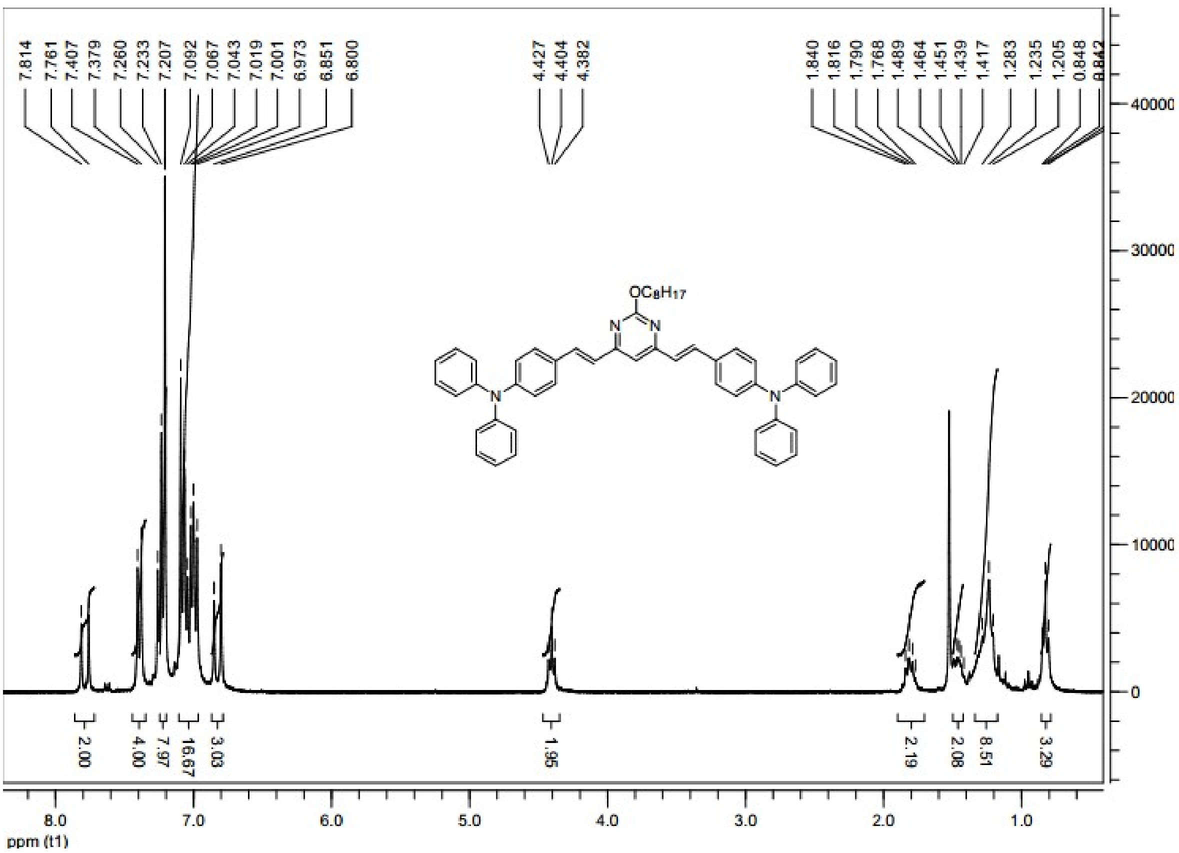

Figure S11. ^{1}H NMR (300 MHz, CDCl$_3$) spectrum of **MOL**.

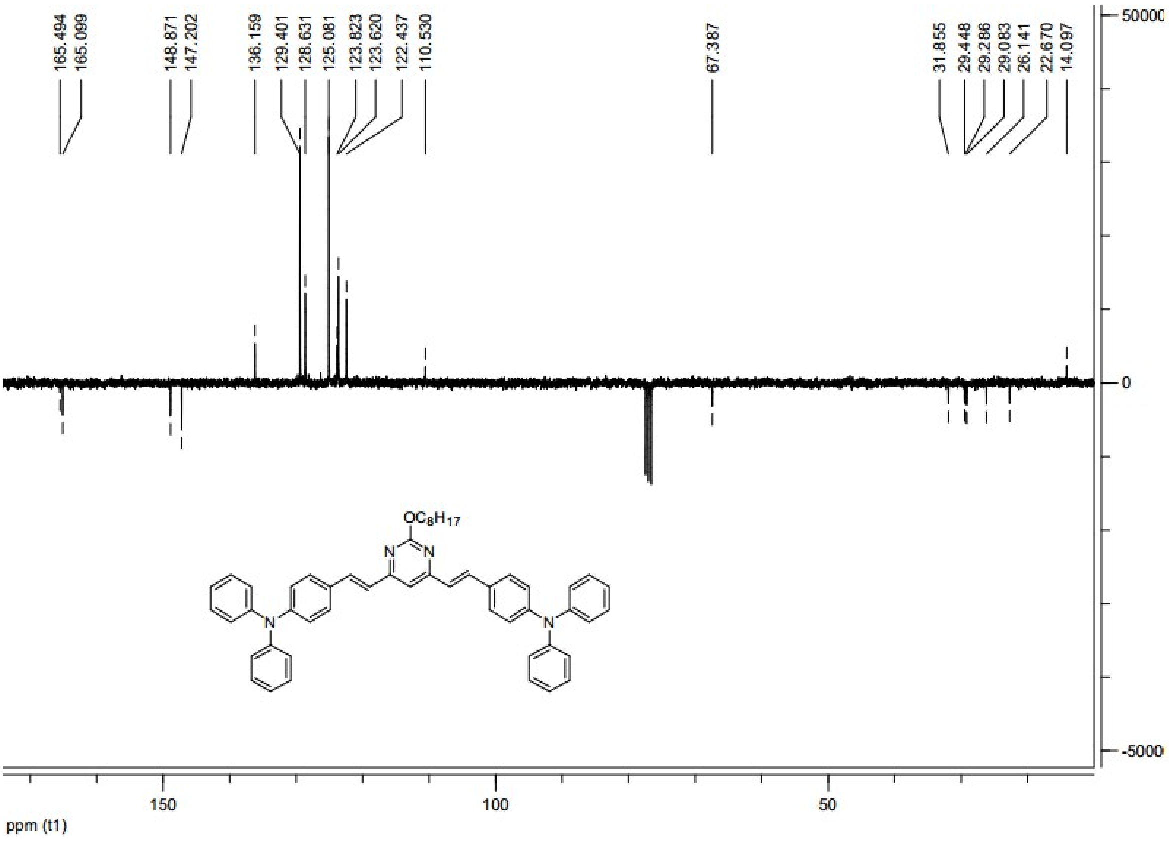

Figure S12. ^{13}C NMR (75 MHz, CDCl$_3$) spectrum of **MOL**

4. References

1 R. Meech and D. Phillips, *J. Photochem.*, 1983, **23**, 193–217.

2 D. V. Connor and D. Phillips, *Time correlated single photon counting* , Academic Press, London, 1984.

3 J.-P. Malval, C. Chaimbault, B. Fischer, J.-P. Morand and R. Lapouyade, *Res. Chem. Interm.*, 2001, **27**, 21-34.

4 I. Horcas, R. Fernandez, J. M. Gomez-Rodriguez, J. Colchero, J. Gomez-Herrero and A. M. Baro, *Rev. Sci. Instrum.*, 2007, **78**, 013705.

5 M. N. Nair, C. Mattioli, M. Cranney, J.-P. Malval, F. Vonau, D. Aubel, J.-L. Bubendorff, A. Gourdon and L. Simon, *J. Phys. Chem. C*, 2015, **119**, 9334-9341.

6 W. Mamdouh, H. Uji-i, J. S. Ladislaw, A. E. Dulcey, V. Percec, F. C. De Schryver and S. De Feyter, *J. Am. Chem. Soc.*, 2006, **128**, 317-325.

7 J.-S. Yang and T. M. Swager, *J. Am. Chem. Soc.*, 1998, **120**, 11864-11873.

8 J.-P. Malval, S. Achelle, L. Bodiou, A. Spangenberg, L. C. Gomez, O. Soppera and F. Robin-Le Guen, *J. Mater. Chem. C*, 2014, **2**, 7869-7880.

9 S. Achelle, I. Nouira, B. Pfaffinger, Y. Ramondenc, N. Plé and J. Rodriguez-Lopez, *J. Org. Chem.*, 2009, **74**, 3711-3717.

ACKNOWLEDGMENTS

The authors acknowledge ‘la Fondation Partenariale Haute-Alsace’ for their funding support.